





Original Article

Role of RNF213 in Guiding Treatment of Moyamoya Disease with Unusual Phenotypic Presentation

Jayanta Roy^{1,†} , Shramana Deb^{1,†} , Ritwick Mondal¹ , Gourav Shome², Bijoy K. Menon³, Ananya Sengupta¹, Nirmalya Ray⁴, Mona Tiwari⁵, Subhadeep Banerjee¹, Avik Mukherjee¹, Sukalyan Purkayastha⁶, Purbita Sen¹, Julián Benito-León^{7,8,9,10} , Mousumi Hazra¹¹ and Saugata Hazra^{12,13}

¹Department of Stroke Medicine, Institute of Neurosciences, Kolkata, India, ²Department of Biological Sciences, Bose Institute, Kolkata, India, ³Department of Clinical Neurosciences, University of Calgary, Alberta, Canada, ⁴Department of Neuroradiology, Manipal Group of Hospitals, Kolkata, India, ⁵Department of Neuroradiology, Institute of Neurosciences, Kolkata, India, ⁶Department of Interventional Neurology, Institute of Neurosciences, Kolkata, India, ⁷Department of Neurology, 12 de Octubre University Hospital, Madrid, Spain, ⁸Instituto de Investigación Sanitaria Hospital 12 de Octubre (imas12), Madrid, Spain, ⁹Centro de Investigación Biomédica en Red Sobre Enfermedades Neurodegenerativas (CIBERNED), Madrid, Spain, ¹⁰Department of Medicine, Complutense University, Madrid, Spain, ¹¹Department of Electrical Engineering, Indian Institute of Technology, Roorkee, India, ¹²Department of Bioscience and Bioengineering, Indian Institute of Technology, Roorkee, India and ¹³Centre for Nanotechnology, Indian Institute of Technology, Roorkee, India

ABSTRACT: Background: Moyamoya disease (MMD) is characterized by progressive carotid fork steno-occlusion and the development of “puff-of-smoke” collaterals on angiography. However, a subset of patients present with similar vascular changes but lack these hallmark collaterals, complicating both diagnosis and management. This “smokeless” phenotype, associated with ring finger protein 213 (RNF213) gene variants, challenges the traditional description of MMD. We describe a series of such patients who responded favorably to revascularization. **Methods:** In this ambispective observational study, we evaluated 12 patients with carotid fork steno-occlusive disease but without “puff-of-smoke” collaterals. Clinical, radiological and genetic assessments were assessed. Structural modeling of RNF213 protein variants was conducted through 3D homology modeling, validated via Ramachandran plots and further refined with COOT and PyMOL. Functional insights were derived through ConSurf analysis. **Results:** Of the 12 patients, 9 carried the RNF213 p.R4810K variant, 1 harboured a novel variant, 1 had both p.R4810K and a novel variant and 1 had p.R4859K. Initial misclassification as intracranial atherosclerosis or vasculitis led to inappropriate treatment. Following genetic confirmation, 9 patients underwent revascularization, with no stroke recurrence and a favorable clinical outcome. Structural modeling revealed minimal functional impact for the Val1529Met variant, whereas other variants significantly disrupted RNF213 stability and functionality. **Conclusions:** “Smokeless moyamoya,” characterized by carotid fork steno-occlusion without typical angiographic collaterals, represents a distinct clinical phenotype responsive to revascularization. RNF213 genetic screening enhances diagnostic precision, reshaping traditional paradigms and supporting tailored therapeutic approaches.

RÉSUMÉ : Le rôle de la protéine RNF213 dans l'orientation du traitement de la maladie de Moya-Moya à phénotype atypique. Contexte : La maladie de Moya-Moya (MMM) se caractérise par la sténose et l'occlusion progressives de la fourche carotidienne et la présence d'un « nuage de fumée » autour des artères collatérales à l'angiographie. Toutefois, dans certains cas, la maladie présente les mêmes changements vasculaires que ceux décrits précédemment mais sans l'image caractéristique des artères collatérales, ce qui complique à la fois le diagnostic et le traitement. Ce phénotype « sans nuage de fumée », associé aux variants génétiques de la protéine à doigts RING 213 (ring finger protein) (RNF213), remet en question la description classique de la MMM. L'article portera donc sur l'état d'une série de patients ayant réagi favorablement à la revascularisation. **Méthode :** Il s'agit d'une étude d'observation ambidirectionnelle, à laquelle ont participé 12 patients ayant une sténo-occlusion de la fourche carotidienne sans « nuage de fumée » des artères collatérales. Les examens cliniques, radiologiques et génétiques ont fait l'objet d'évaluation. La représentation structurale des variants de la protéine RNF213 a été réalisée à l'aide de la modélisation par homologie en 3D, validée avec le diagramme de Ramachandran, puis perfectionnée à l'aide des applications COOT et PyMOL. Enfin, l'idée générale du fonctionnement découle de l'analyse ConSurf. **Résultats :** Sur les 12 patients sélectionnés, 9 étaient porteurs du variant RNF213 p.R4810K; un, d'un tout nouveau variant; un autre, du p.R4810K et d'un tout nouveau variant; et le dernier, du p.R4859K. Des diagnostics d'athérosclérose intracrânienne ou de vascularite, posés à tort initialement ont entraîné des traitements inappropriés. Après confirmation génétique, 9 patients ont subi une intervention de revascularisation, qui a donné lieu à des résultats cliniques satisfaisants, sans récurrence d'accident vasculaire cérébral. La modélisation structurale a révélé une influence fonctionnelle minimale en ce qui concerne le variant Val1529Met, tandis que d'autres perturbaient grandement la stabilité et le fonctionnement de la protéine RNF213. **Conclusion :** La

Corresponding author: Jayanta Roy; Email: jroyneuro01@gmail.com

†: Both these authors contributed equally.

Cite this article: Roy J, Deb S, Mondal R, Shome G, Menon BK, Sengupta A, Ray N, Tiwari M, Banerjee S, Mukherjee A, Purkayastha S, Sen P, Benito-León J, Hazra M, and Hazra S. Role of RNF213 in Guiding Treatment of Moyamoya Disease with Unusual Phenotypic Presentation. *The Canadian Journal of Neurological Sciences*, <https://doi.org/10.1017/cjn.2025.10371>

© The Author(s), 2025. Published by Cambridge University Press on behalf of Canadian Neurological Sciences Federation. This is an Open Access article, distributed under the terms of the Creative Commons Attribution licence (<https://creativecommons.org/licenses/by/4.0/>), which permits unrestricted re-use, distribution and reproduction, provided the original article is properly cited.

présentation de la maladie de Moya-Moya « sans nuage de fumée », qui se caractérise par une sténo-occlusion de la fourche carotidienne mais sans l’image typique des artères collatérales à l’angiographie, constitue un phénotype clinique distinct, qui réagit favorablement à la revascularisation. Le dépistage génétique de la RNF213 améliore la justesse du diagnostic, ce qui donne lieu à une mise à jour des paradigmes habituels et favorise l’individualisation de la démarche thérapeutique.

Keywords: central nervous system vasculitis; clinical exome sequencing; carotid fork; moyamoya disease; moyamoya syndrome; primary angiitis of the central nervous system; stroke; smokeless moyamoya; ring finger protein 213

(Received 24 April 2025; final revisions submitted 17 June 2025; date of acceptance 9 July 2025)

Highlights

- Moyamoya disease (MMD) can present without the “puff-of-smoke” collaterals (smokeless), resembling moyamoya syndrome.
- Genetic testing for RNF 213 assists in identifying the smokeless MMD variant and directs treatment.
- Structural modeling shows variant-specific RNF213 disruptions that impair angiogenesis, highlighting its role in “smokeless” MMD expression.

Background

Moyamoya disease (MMD) is an idiopathic, sometimes familial condition characterized by progressive steno-occlusion of the distal internal carotid arteries (ICAs) and circle of Willis, often involving the carotid fork (distal to the anterior choroidal arteries).¹ Its hallmark is a network of basal collaterals resembling a “puff-of-smoke” on angiography, as described by Suzuki and Takaku in 1969 based on 20 cases. The Suzuki staging system (I–VI), derived from serial angiograms of four young patients, remains a cornerstone of MMD classification.² Conditions mimicking MMD, collectively termed moyamoya syndrome (MMS) or quasi-moyamoya, include central nervous system vasculitis, intracranial atherosclerosis, sickle cell disease and varicella zoster vasculitis (Table 1).³

In patients presenting with steno-occlusive changes at the carotid fork but lacking the characteristic “puff-of-smoke” collaterals, there is a tendency to pursue extensive investigations and initiate empirical treatments for MMS. This approach may lead to unnecessary or even harmful interventions. Recognizing that such presentations can still represent MMD, particularly in the presence of RNF213 gene mutations, underscores the importance of incorporating genetic testing into the diagnostic process. Early identification through genetic studies can prevent misdiagnosis, reduce unwarranted treatments and facilitate appropriate management strategies.

We have identified a subset of patients exhibiting unilateral or bilateral, often asymmetric, steno-occlusive changes at the carotid fork without the hallmark “puff-of-smoke” angiographic collaterals. This absence frequently leads to diagnostic ambiguity, prompting extensive investigations and empirical treatments for MMS, which may be unnecessary or even detrimental. Notably, clinical exome sequencing targeting the RNF213 gene has clarified these diagnostic challenges, aligning with cases such as that reported by Morikawa et al., where a 40-year-old Chinese woman was initially misdiagnosed with primary angiitis of the central nervous system (PACNS) but was later correctly identified as having MMD with the p.R4810K variant and subsequently improved following revascularization.⁴ To better characterize this distinct clinical entity, we propose the term “smokeless

moyamoya,” acknowledging its divergence from classic MMD presentations. In this study, we detail the clinical, radiological and genetic profiles of these patients, assess their treatment outcomes and explore the structural implications of RNF213 variants to elucidate the molecular underpinnings of this phenotype.

Methods

Ethics statement

This study adhered to the Declaration of Helsinki principles. All participants, or a parent/guardian for minors, provided written informed consent. The Institutional Ethics Committee approved the study with reference number INK/COP/FM/05. Additionally, participants consented to genetic analysis per the Indian Council of Medical Research ethical guidelines (2017, section 10.4.5) .

Study design and selection of participants

We conducted an ambispective observational study at our institute from March 2021 to January 2025, screening all stroke unit patients with ischemic stroke or atypical intracerebral hemorrhage (with or

Table 1. Illustrates the angiographic mimics of moyamoya and demonstrates the diagnostic criteria of primary angiitis of the central nervous system (PACNS)

Angiographic mimic of moyamoya
1. Intracranial atherosclerotic disease
2. CNS vasculitis
3. Sickle cell disease
4. Varicella vasculopathy
5. Radiation vasculopathy
6. Fibromuscular dysplasia
7. Arterial dissection
8. Down syndrome
9. Neurofibromatosis type 1
10. Reversible cerebral vasoconstriction syndrome
Calabrese and Mallek’s criteria have to be met for the definite diagnosis of PACNS
1. History and clinical features of an acquired neurological deficit that remains unexplained after a proper initial basic evaluation consisting of blood counts, blood biochemistry, CSF studies, neuroimaging, and serological tests.
2. Either classic angiographic or biopsy features of angiitis of the central nervous system.
3. No evidence of systemic vasculitis or any other condition to which the angiography or histopathology could be attributed.

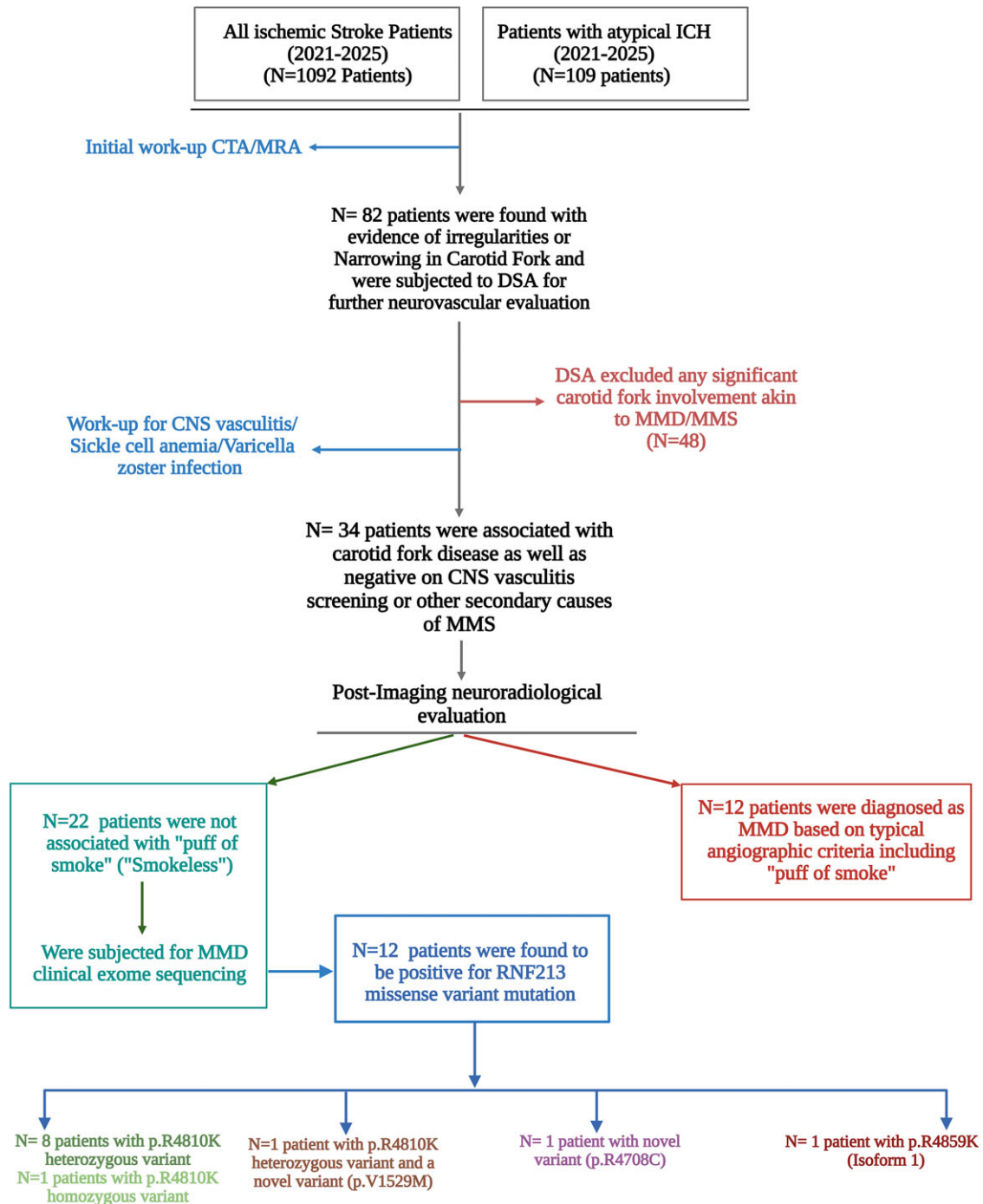


Figure 1. Flow chart of the study participants' selection criteria. ICH = intracerebral hemorrhage; CTA = CT angiography; MRA = MR angiography; DSA = digital subtraction angiography; MMS = moyamoya syndrome; MMD = moyamoya disease; RNF213 = ring finger protein 213.

without intraventricular extension). Participants were selected based on (1) carotid fork narrowing or irregularities on CT/MR angiography, (2) negative systemic vasculitis screening, (3) no sickle cell anemia or infections (varicella zoster, HIV, hepatitis B/C, syphilis), (4) normal CSF analysis, (5) absence of "puff-of-smoke" collaterals on digital subtraction angiography (DSA) and (6) presence of RNF213 missense variants. Selected patients were prospectively followed for treatment and outcomes (Figure 1). Those with compound heterozygous RNF213 variants were excluded. The study's reporting system followed the STROBE

guidelines (Strengthening the Reporting of Observational Studies in Epidemiology)⁵ (Supplementary file).

Baseline data collection

We collected demographic data, vascular risk factor history, clinical characteristics and laboratory parameters. Neurological status was assessed using the Glasgow Coma Scale (GCS), National Institutes of Health Stroke Scale (NIHSS) and modified Rankin Scale (mRS). Peripheral blood samples were analyzed for

Table 2. Baseline demographic characteristics, clinical presentation and biochemical analysis

Parameters	Patient ID											
	001	002	003	004	005	006	007	008	009	010	011	012
Age	68Y	46Y	42Y	49Y	38Y	39Y	48Y	51Y	28Y	31Y	56Y	36Y
Age at onset	68 (for the past 1 month)	45.5Y (for the last 5–6 months)	41.6Y	49Y (first ever presentation)	38Y (past 2 months)	39Y/F (for the last 3 months with HX of Recurrent left hemispheric TIA)	48Y (for the past 3 months)	50.5Y/F (for the last 4–5 months)	28Y	30.5 y (for the past 6–7 months)	56Y	35Y (for 1 year)
Sex	Female	Female	Female	Female	Male	Female	Female	Female	Female	Female	Male	Female
Vascular risk factors	Hypertension, T2 DM, obesity	Hypertension, T2 DM (for last 7 years), obesity	Hypertension, T2 DM, obesity	T2 DM, hypertension, dyslipidemia Increased serum homocysteine level	Hypertension, T2 DM (past 12 years), Hypothyroidism	Hypothyroidism	T2 DM	Hypothyroidism, Hypertension	Hypothyroidism	Hypertension, Hypothyroidism	Hypertension, T2 DM, Increased serum homocysteine level	Hypothyroidism (for the last 7 years)
Baseline neurological presentation	-Acute onset deviation of angle of mouth on left -Left-sided hemiparesis (one month before) -Plantar reflex Decreased B/L -GCS 15/15 (E4V5M6) -NIHSS 5 -mRS 3	-Right-sided deviation of angle of mouth -Left UL weakness -Sudden onset slurring of speech -Plantar left (extensor) and right (flexor) -GCS 15/15 (E4V5M6) -NIHSS 6 -mRS 3	-Left UL weakness due to left-UMN facial palsy -Left hemiparesis -Tingling sensation and numbness in left UL -Dysarthria -Seizure -DTR- decreased on left plantar left extensor, right flexor -GCS 15/15 (E4V5M6) -NIHSS 6 -mRS 3	-Slight deviation of face toward left (24 h) -Drooling of saliva -Acute onset of unsteadiness -1 episode of seizure -Headache -Plantar B/L flexor -GCS 15/15 (E4V5M6) -NIHSS 0 -mRS 1	-Tingling sensation of right UL -Headache with vomiting -Bowel and bladder incontinence -Gradually diminishing sensation of B/ L LL up to the level of the umbilicus -Plantar (B/L decreased) -GCS 15/15 (E4V5M6) -NIHSS – 0 -mRS 2	-Occasional events of right-sided weakness with tingling sensation -Aphasia (for last 3 months) -Recurrent left hemispheric TIA -GCS 15/15 (E4V5M6) -NIHSS 6 -mRS 3	-Persistent low-grade headache -Gradually diminishing vision in both eyes (left>right) (since past 2–3 months) -Gait - mild unsteadiness -Recurrent stroke syndrome -GCS 15/15 (E4V5M6) -NIHSS 4 -mRS 3	-Acute onset slurring of speech with the inability to perform everyday tasks x 8 days -DTR 3+ B/L plantar flexors + -Recurrent TIA -GCS 15/15 (E4V5M6) -NIHSS 4 -mRS 2	-Sudden onset left-sided hemiparesis -DTR- exaggerated -Plantar - B/L Flexor decreased -GCS 5/5 (E4V5M6) -NIHSS 6 -mRS 3	-Right-sided deviation of angle of mouth -weakness and numbness over right hand (for past 6–7 months) -One episode of afebrile convulsion -Multiple episodes of LOC -DTR + -GCS 15/15 (E4V5M6) -NIHSS 0 mRS 2	-Facial deviation lasting about a minute -GCS 15/15 (E4V5M6) -NIHSS 2 mRS 2	-Sudden onset right-sided hemiparesis -Dysarthria -GTCS -GCS 15/15 (E4V5M6) -NIHSS-5 mRS 3
Stroke pattern on evaluation	Bilateral MCA territorial hypoperfusion due to multiple luminal stenosis.	Right-sided thalamic infarction (on NCCT) with the right MCA territorial involvement/ hypoperfusion	Recurrent Right MCA territory infarction	Right MCA territorial infarction	Acute infarction over left FTP area with B/L cortical involvement	Left hemispheric TIA with hypoperfusion	Right PCA territorial infarction	Right MCA territorial infarction, Recurrent episodes of infarction due to large vessel occlusion	Right-sided MCA territorial infarction/ hypoperfusion	Left MCA territorial ischemic changes / hypoperfusion	Right-sided MCA territorial infarction	Left-sided MCA territorial ischemic CVA
Serum parameters												
Platelet count (L)	2.1	1.67	1.6	2.73	1.6	1.78	1.8	2.3	3.25	2.52	1.7	2.3
Prothrombin time (PT) (sec)	13.5	12.1	14.2	11.4	10.8	11.4	11.9	13.5	10.7	12	12.6	12.4
Bleeding time (sec)	2.52	2.34	2.21	2.27	2.46	2.38	2.62	2.55	2.21	2.18	2.20	2.62

Table 2. Baseline demographic characteristics, clinical presentation and biochemical analysis (*Continued*)

Parameters	Patient ID											
Clotting time (sec)	5.05	5.1	4.50	4.8	5.28	5.32	5.15	4.56	5.24	4.75	4.5	4.6
Activated partial thromboplastin time (aPTT) (sec)	28.7	30.5	28.5	30.7	27.2	26.7	28.5	28.5	27.7	28.6	30.3	30.5
International Normalized Ratio	0.9	1.06	1.05	0.96	1.08	0.89	1.13	1.02	0.90	1.12	1.06	0.94
WBC (cells/ μ L)	5800	13,200	10,100	9700	6200	7800	6200	7700	14,500	8300	11,100	5400
ESR (mm/h)	20	31	25	83	26	28	22	25	83	32	20	19
CRP (mg/dL)	5.4	6.2	12	27	5.8	4.9	2.4	2.6	19	6.6	0.7	3.8
Na ⁺ (mEq/L)	138	136	139	135	140	134	135	144	139	142	139	141
K ⁺ (mEq/L)	4.7	3.6	4	3.9	4.2	3.8	3.9	4.2	4.6	4.5	3.9	4
Creatinine (mg/dL)	0.64	0.9	0.55	1.31	1.05	0.65	0.52	0.74	0.79	0.78	0.51	0.96
LDL (mg/dL)	108	106	108	110	104	100	101	103	103	107	103	108
HDL (mg/dL)	47	40	45	49	45	44	51	43	57	47	40	45
LDL/HDL	2.29	2.65	2.50	2.24	2.31	2.27	2	2.39	1.8	2.27	2.5	2.8
Homocysteine (μ mol/L)	12.8	13.2	15.2	16	14.7	12.6	11.7	15	11.3	12.5	16.2	14.6
CSF vasculitis panel	Negative	Negative	Negative	Negative	Negative	Negative	Negative	Negative	Negative	Negative	Negative	Negative

TIA = transient ischemic attack; HX = History; B/L = bilateral; GCS = Glasgow Coma Scale; mRS = modified Rankin Scale; NIHSS = National Institutes of Health Stroke Scale; MCA = middle cerebral artery; ICA = distal internal carotid artery; PCA = posterior cerebral artery; NCCT = contrast CT; CRP = C-reactive protein; LDL = low-density lipoprotein; HDL = high-density lipoprotein; T2 DM = Type 2 diabetes mellitus; UL = upper limb; LL = lower Limb; UMN = upper motor neuron; DTR = deep tendon reflex; ESR = erythrocyte sedimentation rate; CVA = cerebrovascular attack; FTP = frontotemporoparietal; GTCS = generalized tonic clonic seizure; LOC = loss of consciousness.

Table 3. Anatomical site-specific involvement of the carotid fork in patients with “smokeless moyamoya”

Patient ID	Anatomical site of intra-cranial arterial involvement			
	Terminal ICA	Proximal MCA	Proximal ACA	Other vascular findings
001	NA	B/L symmetrical narrowing in M1-MCA	NA	NA
002	B/L narrowing in the right and left supraclinoid segments of ICA	NA	NA	NA
003	Narrowing in right-sided supraclinoid ICA	B/L narrowing in M1-MCA	B/L narrowing in A1-ACA	Right P2-PCA narrowing
004	Narrowing in right-sided supraclinoid ICA	Narrowing in right M1-MCA	B/L narrowing in A1-ACA	Right MCA-PCA pial-pial collaterals
005	B/L narrowing of the cavernous segment of ICA	NA	NA	Filling of left MCA from PCOM due to proximal occlusion within the ipsilateral ICA
006	NA	Narrowing in left M1-MCA	NA	NA
007	B/L narrowing terminal segments of ICA	B/L narrowing in M1-MCA	B/L narrowing in A1-ACA	Right-sided PCA occlusion beyond P1, left P2-PCA narrowing, left PCA-MCA pial collaterals
008	B/L narrowing in supraclinoid segments of ICA	B/L narrowing in M1-MCA	NA	B/L narrowing at P1-P2 junction of PCA
009	NA	B/L narrowing in M1-MCA	NA	NA
010	-Mild narrowing in right: ICA origin -Significant narrowing in left ICA origin	Narrowing in left-sided M1-MCA	Narrowing in left-sided A1-ACA	NA
011	NA	B/L narrowing in M1-MCA	NA	NA
012	NA	B/L narrowing in M1-MCA	NA	NA

ICA = distal internal carotid artery; MCA = middle cerebral artery; ACA = anterior cerebral artery; PCA = posterior cerebral artery; PCOM = posterior communicating artery; B/L = bilateral; NA = not applicable.

biochemical, serological and immunological profiles using enzymatic methods.

Neuroradiological evaluation and assessment of angiographic landscape

Imaging protocol

Initial neuroimaging for all stroke patients followed institutional protocol, using non-contrast CT (NCCT) and CT angiography (CTA) or MRI and MR angiography (MRA). MRI was performed on 1.5- or 3.0-Tesla machines. In select cases, single-photon emission computed tomography with Technetium-99 m ethyl cysteinate dimer assessed regional blood flow and cerebrovascular reactivity before extracranial-intracranial (EC-IC) bypass surgery. Additional modalities included high-resolution vessel wall imaging (HR-VWI) and six-vessel cerebral DSA. Pre-DSA screening measured urea and creatinine levels. DSA, conducted on a flat-panel detector system (Artis Zee Floor, Siemens, Germany), involved bilateral super-selective catheterization of the common carotid, external carotid, internal carotid and vertebral arteries via femoral puncture, with contrast injection (5 mL/s) and multi-angle visualization (1024 × 1024 matrix, 22-cm field of view and 0.21 × 0.21-mm pixel size).

Post-neuroimaging data analysis

Post-imaging, 3D and 4D analyses generated virtual reality (VR) and maximum intensity projection (MIP) images. From DSA, 18 phases – including arterial, arteriovenous and venous – were

selected for optimal segmentation, cutting and reconstruction quality. VR and MIP images depicted the siphon and bifurcation of the bilateral ICAs, anterior, middle and posterior cerebral arteries, vertebrobasilar system and circle of Willis. The arterial phase was further analyzed in anteroposterior, posteroanterior, left-lateral and right-lateral views for all patients.

Deoxyribonucleic acid sequencing and data analysis

Clinical exome sequencing by next-generation sequencing

Deoxyribonucleic acid (DNA) was extracted from peripheral blood using a Qiagen isolation kit. Libraries were prepared per the SureSelect XTBS2 protocol and sequenced on the Illumina NovaSeq 6000 platform. Demultiplexing generated FastQ files, and raw reads underwent quality control with FastQC v0.12.1. High-quality reads were mapped to the hg38 reference genome (GRCh38) using BWA-MEM. Variant calling, including single nucleotide variants and small insertions/deletions (InDels), was performed with GATK-v4.3 and the SMART-One™ Tech Platform, following best-practice workflows.

Multiple sequence alignment and pathogenicity score analysis

Conservation analysis of amino acid residues for RNF213 variants was performed using the UniProtKB/Swiss-Prot database and BLASTp, with hg38 as the reference genome. Variant pathogenicity and deleterious effects were assessed using bioinformatics tools, including Polyphen2,⁶ PANTHER-PSEP,⁷ ClinVar⁸ and CADD.⁹

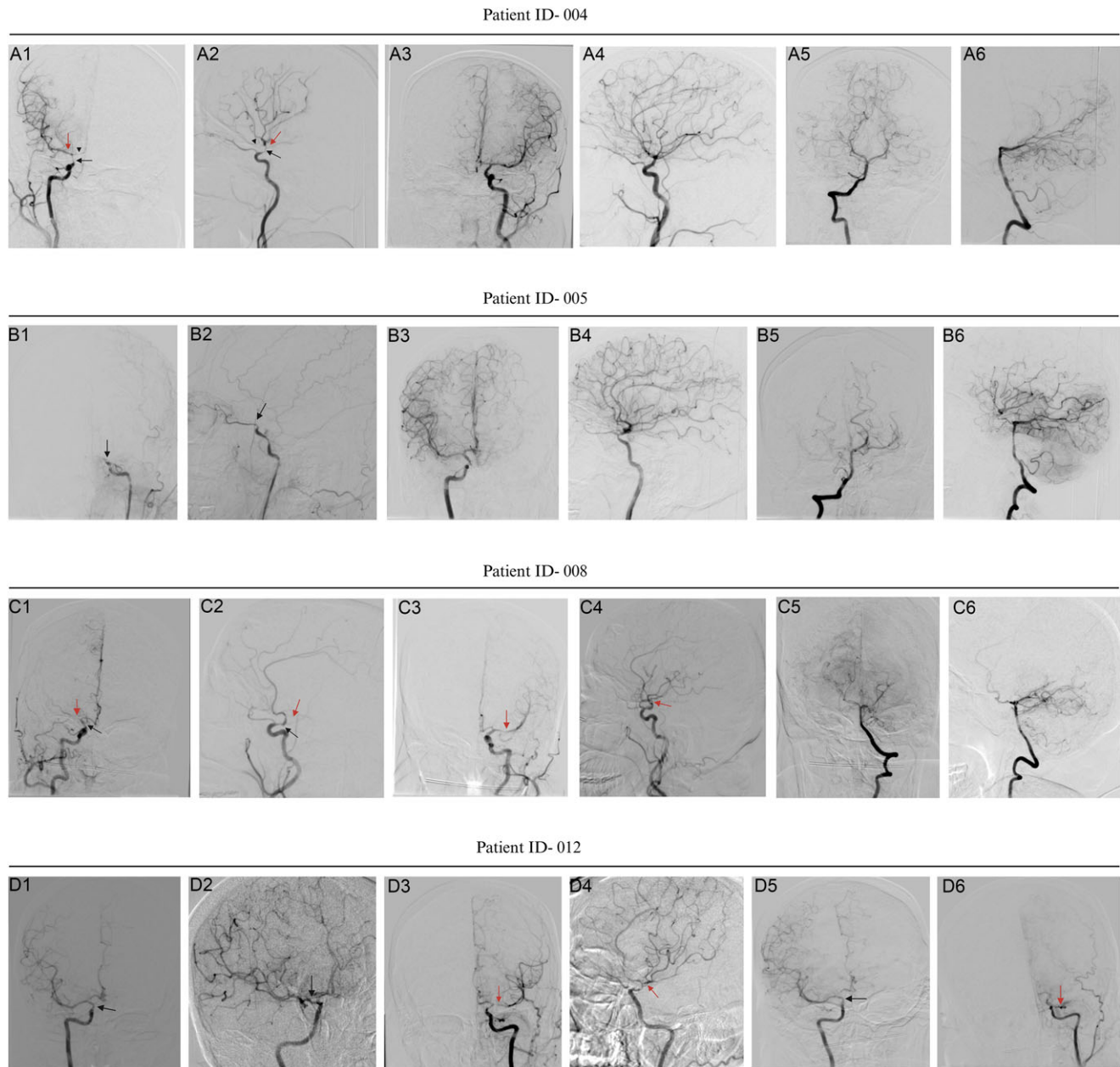


Figure 2. (A1) and (A2) The right internal carotid artery angiogram in the anteroposterior and lateral projections shows abrupt narrowing involving the supraclinoid segment (black arrow) of the right internal carotid artery, with a thread-like appearance of the supraclinoid segment of the right internal carotid artery. Marked narrowing of the A1 segment of the right anterior cerebral artery (arrowhead) is also noted. The M1 segment of the right middle cerebral artery appears beaded (red arrow) with mild narrowing at places. However, the distal branches of the right middle cerebral artery show normal caliber and contrast opacification. (A3) and (A4) with left internal carotid artery injection in anteroposterior and lateral projection show normal caliber and contrast opacification of the left internal carotid artery, left middle cerebral artery, left anterior cerebral artery, left vertebral artery, basilar artery and bilateral posterior cerebral arteries. Note the filling of the A2 segment of the right anterior cerebral artery and its branches through the anterior communicating artery on the left internal carotid artery injection. (B1) and (B2) Left internal carotid artery angiogram in the anteroposterior and lateral projections shows chronic complete total occlusion of the supraclinoid segment (black arrow) of the left internal carotid artery after the origin of the left ophthalmic artery. (B3) and (B4) Right internal carotid artery injection in anteroposterior and lateral projection showing normal caliber and contrast opacification of the right internal carotid artery, right anterior and right middle cerebral artery, and their branches. The A2 segment of the left anterior cerebral artery and the distal left anterior cerebral artery branches are normally opacified on the right internal carotid artery injection through the anterior communicating artery. (B5) and (B6) Right vertebral artery injection in anteroposterior and lateral projection shows near-complete reformation of the M1 segment of the left middle cerebral artery and its distal branches. However, no evidence of the typical “puff-of-smoke” appearance was seen. (C1) and (C2) Right internal carotid artery angiogram in the anteroposterior and lateral projections shows a moderate abrupt narrowing in the supraclinoid segment (black arrow) of the right internal carotid artery, with non-opacification of the M1 segment of the right middle cerebral artery (red arrow). (C3) and (C4) Left internal carotid artery injection in anteroposterior and lateral projection showing a moderate narrowing in the mid to distal M1 segment of the left middle cerebral artery (red arrow) without any obvious narrowing of the supraclinoid segment of the left internal carotid artery. (C5) and (C6) Left vertebral artery injection in anteroposterior and lateral projection shows partial reformation of the right hemi-anterior circulation via the posterior communicating artery and a few pial-pial collaterals from the right posterior cerebral artery branches. However, the typical “puff-of-smoke” appearance was not seen. (D1) and (D2) Right internal carotid artery angiogram in the anteroposterior and right anterior oblique projections showing a mild narrowing in the supraclinoid segment of the right internal carotid artery (black arrow). (D3) and (D4) Left internal carotid artery injection in anteroposterior and lateral projection showing moderate narrowing involving the supraclinoid segment of the left internal carotid artery with narrowing of the M1 segment of the left middle cerebral artery (red arrow). No evidence of abnormal collaterals or typical “puff-of-smoke” appearance was noted. (D5) and (D6) show serial DSA done after six months. (D5) shows a right internal carotid artery angiogram in anteroposterior projection with a mild increase in the narrowing in the supraclinoid segment of the right internal carotid artery (black arrow). (D6) Left ICA angiogram on anteroposterior projection shows occluded M1 segment of the left middle cerebral artery, with accentuation of the narrowing in the supraclinoid segment of the left internal carotid artery (red arrow). However, even on the serial DSA, abnormal collaterals or typical “puff-of-smoke” appearances are not appreciated.

Table 4. Genetic landscape of the 12 included patients with the “smokeless moyamoya phenotype”

Patient ID	Gene and transcript	Isoform	Exon	Chromosomal position	Ref allele	Altered allele	Genetic variants	Protein variants	Variant Type	rsID	Zygosity
001	RNF213 NM_001256071.3	Isoform 3	60	Chr17:80385145	G	A	c.14429G>A	[p. Arg4810Lys]	Missense	rs112735431	Heterozygous
002	RNF213 NM_001256071.3	Isoform 3	60	Chr17:80385145	G	A	c.14429G>A	[p. Arg4810Lys]	Missense	rs112735431	Heterozygous
003	RNF213 NM_001256071.3	Isoform 3	60	Chr17:80385145	G	A	c.14429G>A	[p. Arg4810Lys]	Missense	rs112735431	Heterozygous
004	RNF213 NM_001256071.3	Isoform 3	60	Chr17:80385145	G	A	c.14429G>A	[p. Arg4810Lys]	Missense	rs112735431	Heterozygous
005	RNF213 NM_001256071.3	Isoform 3	59	Chr17:80383728	C	T	c.14122C>T	[p. Arg4708Cys]	Missense	rs367968390	Heterozygous
006	RNF213 NM_001256071.3	Isoform 3	60	Chr17:80385145	G	A	c.14429G>A	[p. Arg4810Lys]	Missense	rs112735431	Heterozygous
007	RNF213 NM_001256071.3	Isoform 3	60	Chr17:80385145	G	A	c.14429G>A	[p. Arg4810Lys]	Missense	rs112735431	Heterozygous
008	RNF213 NM_001256071.3	Isoform 3	60	Chr17:80385145	G	A	c.14429G>A	[p. Arg4810Lys]	Missense	rs112735431	Heterozygous
	RNF213 NM_001256071.3	Isoform 3	24	Chr17:80337643	G	A	c.4585G>A	[p. Val1529Met]	Missense	Not reported	Heterozygous
009	RNF213 NM_001256071.3	Isoform 3	60	Chr17:80385145	G	A	c.14429G>A	[p. Arg4810Lys]	Missense	rs112735431	Heterozygous
010	RNF213 NM_001256071.3	Isoform 3	60	Chr17:80385145	G	A	c.14429G>A	[p. Arg4810Lys]	Missense	rs112735431	Homozygous
011	RNF213 NM_001256071.3	Isoform 3	60	Chr17:80385145	G	A	c.14429G>A	[p. Arg4810Lys]	Missense	rs112735431	Heterozygous
012	RNF213 NM_001410195.1	Isoform 1	61	Chr17:80385145	G	A/C	c.14576G>A	[p. Arg4859Lys]	Missense	rs112735431	Heterozygous

Methods of revascularization

Revascularization employed direct methods, such as EC-IC bypass (superficial temporal artery to middle cerebral artery [MCA]), and indirect methods, including encephalo-duro-arterio-myo-synangiosis (EDAMS) and/or encephalo-duro-arterio-synangiosis. The neurosurgical team determined the appropriate approach (direct, indirect or combined).

Follow-up

We recorded stroke recurrence and mRS scores at the longest post-surgical follow-up interval of 24 months.

Statistical analysis

Statistical analyses were conducted using IBM SPSS Statistics for Windows, Version 26.0. A complete case analysis approach was employed. Categorical variables are presented as frequencies and percentages, while continuous variables are summarized using means and standard deviations (SD).

Structural modeling and variant generation of E3 ubiquitin-protein ligase RNF213

The E3 ubiquitin-protein ligase RNF213 (Isoform 3, UniProt ID: Q63HN8), a 5,207-amino-acid protein, was modeled using homology modeling. Its sequence was sourced from UniProt, and a BLAST search identified the cryo-EM structure (PDB ID:

8S24) as the optimal template based on structural and functional similarity.^{10–11} Template gaps, corresponding to missing residues (Supplementary file), were reconstructed via loop modeling in Modeler 9.2. The structure was refined with SWISS-MODEL, followed by energy minimization in GROMACS (50,000 steepest descent steps) and a 300-ps molecular dynamics simulation to ensure stability.^{12–14} Model validation used Ramachandran plot analysis in PDBSUM to confirm phi-psi angle conformity.¹⁵ Three variants – Val1529Met, Arg4708Cys and Arg4810Lys – were generated using COOT for refinement and PyMOL for visualization and mutagenesis.¹⁶ Evolutionary conservation was assessed with ConSurf, highlighting critical structure-function regions.¹⁷ This workflow produced a robust RNF213 model and its variants, offering insights into its structural and functional roles.

Results

Demographic and clinical characteristics (Table 2)

The cohort comprised 12 patients with a mean age of 44.3 years (SD ± 11.1). The majority were female (83.3%, $n = 10$), with males representing 16.7% ($n = 2$). Prevalent vascular risk factors included arterial hypertension (66.7%, $n = 8$), diabetes mellitus (58.3%, $n = 7$), hypothyroidism (50.0%, $n = 6$), obesity (33.3%, $n = 4$) and dyslipidemia (8.3%, $n = 1$). These risk factors were more commonly observed among females aged 31–60 years. Additionally, elevated serum homocysteine levels were identified in 16.7% of patients ($n = 2$).

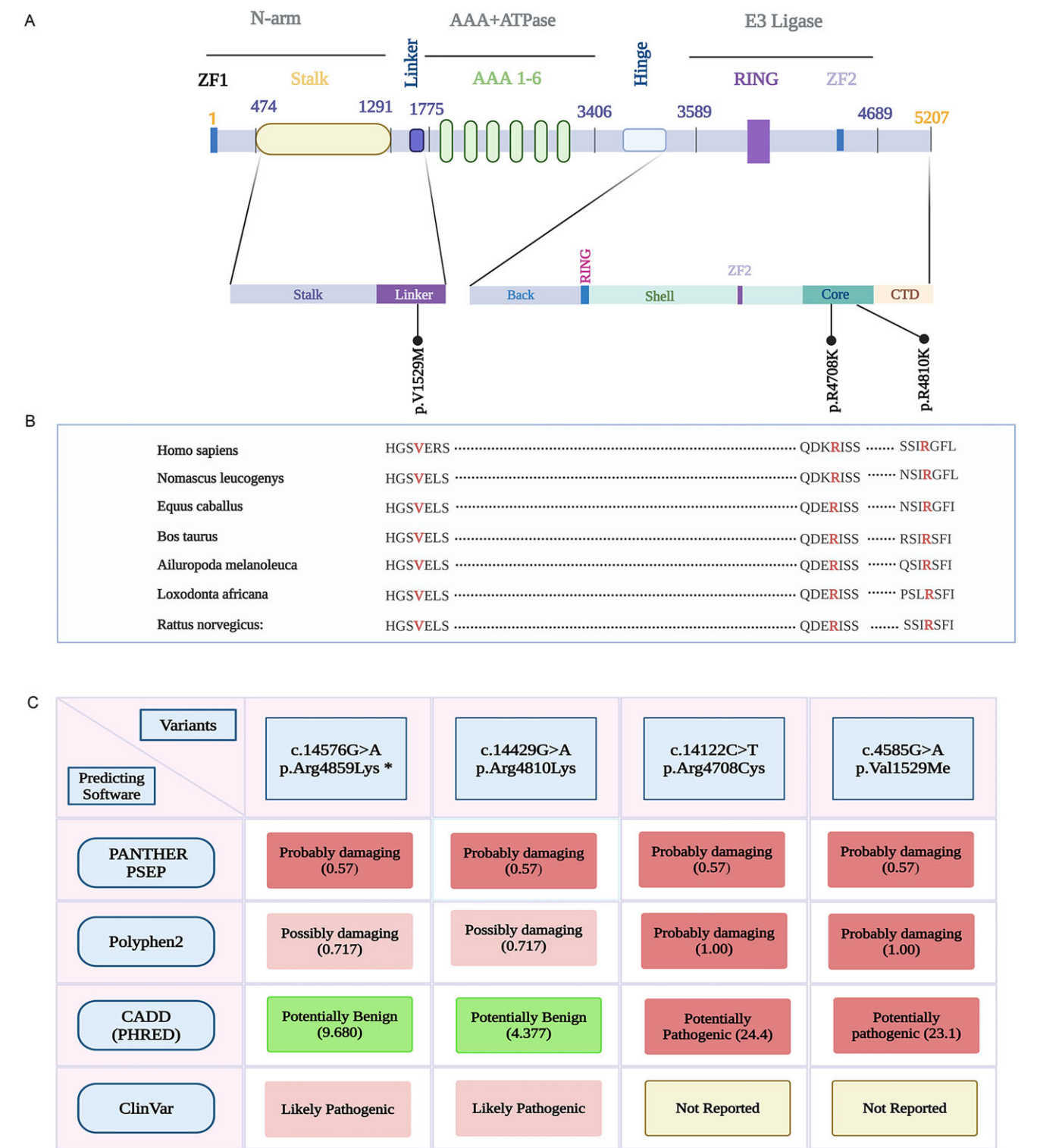


Figure 3. (A) Variants identified in the study and their relative position across different domains of RNF213 (Isoform 3). (B) Conservation of the amino acid residues in RNF213 in correspondence to the above-reported variants. (C) Pathogenic characteristics of the identified RNF213 variants through different predicting software. ZF = zinc finger; AAA = ATPase associated with various cellular activities; PANTHER PSEP = protein analysis through evolutionary relationship - position-specific evolutionary preservation; Polyphen 2 = Polymorphism Phenotyping v2; CADD (PHRED) = Combination Annotated Dependent Depletion; ClinVar = clinical variant.

Neurological presentation and stroke characteristics (Table 2)

Among the 12 patients in the cohort, 33.3% ($n = 4$) presented with a baseline NIHSS score ≥ 6 , indicating moderate to severe stroke

severity, and 83.3% ($n = 10$) had an mRS score ≥ 2 , reflecting at least slight disability.

Common clinical presentations included facial palsy or weakness in 50% of patients ($n = 6$), hemiparesis in 41.7% ($n = 5$) – predominantly left-sided – and dysarthria in 41.7% ($n = 5$). Other

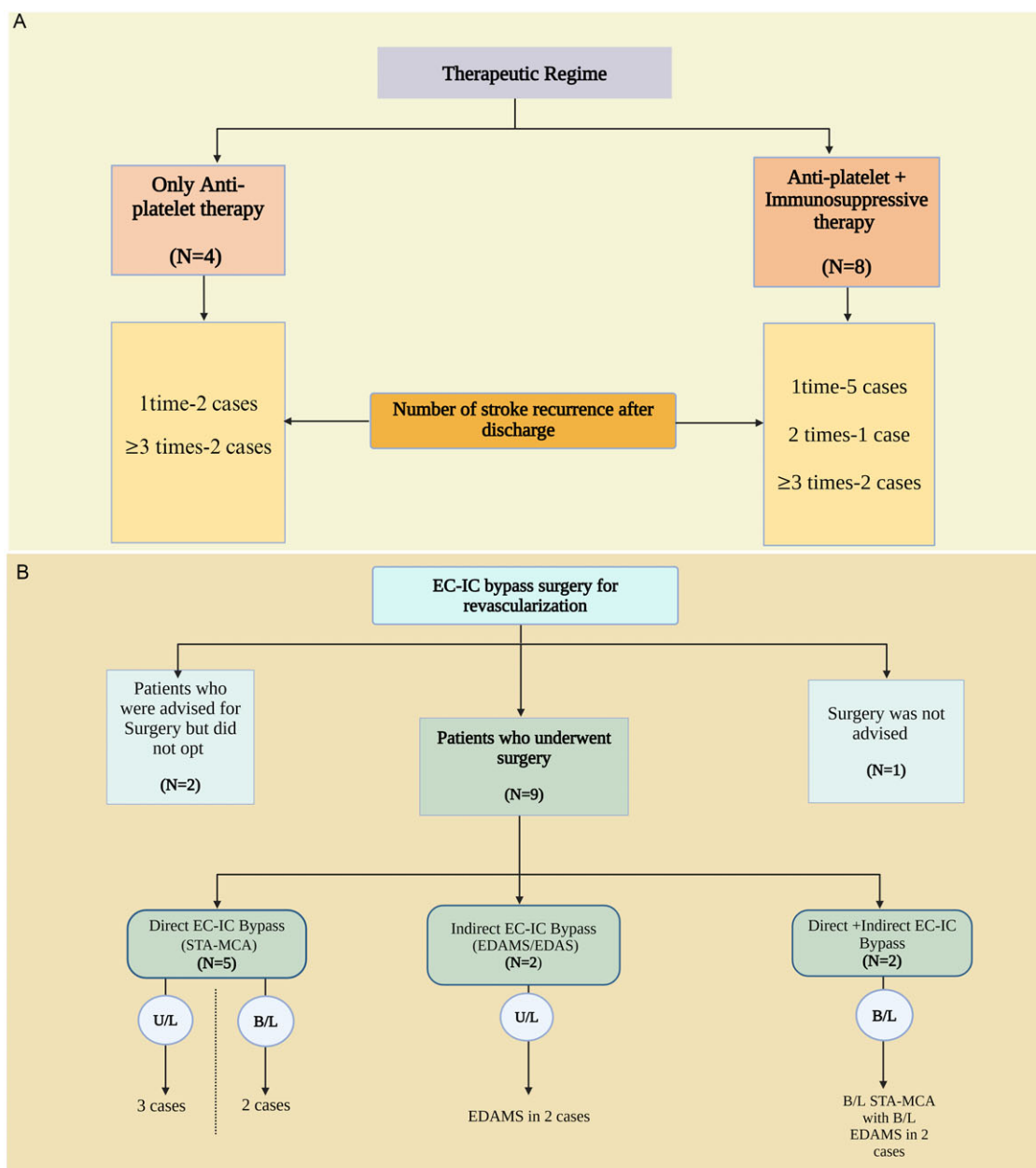


Figure 4. Treatment and follow-up: (A) Illustrates the two primary therapeutic regimens given to the patients after their baseline presentation. It also shows the recurrence of ischemic events related to each treatment group following discharge and during later follow-up visits. (B) Demonstrates the patients' decisions and demographic summary in correspondence with revascularization surgical procedures. EC-IC = extracranial-intracranial; STA-MCA = superficial temporal artery-middle cerebral artery; EDAMS = encephalo-duro-arterio-myo-synangiosis; EDAS = encephalo-duro-arterio-synangiosis; U/L = unilateral; B/L = bilateral.

symptoms comprised seizures (33.3%, $n = 4$), increased deep tendon reflexes (33.3%, $n = 4$), decreased plantar reflexes (25.0%, $n = 3$), gait disturbances (25.0%, $n = 3$), headache (25.0%, $n = 3$) and sensory deficits (25.0%, $n = 3$). Vision loss was reported in one patient.

All patients experienced ischemic symptoms. Two patients had transient ischemic attacks, including one with recurrent left hemispheric events. Notably, one patient (ID-07) experienced more than six stroke recurrences.

Infarcts predominantly involved the MCA territory, observed in 91.7% of patients ($n = 11$). Among these, right-sided infarcts were most common (63.6%, $n = 7$), followed by left-sided (27.3%, $n = 3$) and bilateral involvement (9.1%, $n = 1$). One patient exhibited an infarct in the posterior cerebral artery territory.

Baseline biochemical parameters (Table 2)

All 12 patients underwent comprehensive biochemical profiling, including assessments of coagulation, metabolic, vascular, electrolyte, inflammatory, hemoglobinopathy, thyroid function and markers pertinent to PACNS, in accordance with European Stroke Organisation guidelines. No single parameter definitively indicated PACNS. Routine laboratory tests – including complete blood count, electrolytes, coagulation profile, lipid panel, liver and renal function tests – were within normal limits. CSF analyses revealed normal leukocyte counts, protein and glucose levels, effectively excluding infectious or neoplastic etiologies. Mean C-reactive protein (CRP) levels were elevated (8.02 ± 2.2 mg/dL), and low-density lipoprotein cholesterol levels were slightly raised

Patient ID	Age/Sex	Treatment Offered		Recurrence (Number of Stroke Events)	Surgery offered	Opted for Surgery (✓/✗)	Follow-up (mRS) (↓/↑)
		Anti-Platelet	Immunosuppressive Therapy				
001	68Y/F	✓	✓	○	Not Suggested	NA	3 (Unchanged)
002	46Y/F	✓	✗	○	✓	✓	2 ↓
003	42Y/F	✓	✓	○○	✓	✗	4 ↑
004	49Y/F	✓	✓	○	✓	✓	1 (Unchanged)
005	38Y/M	✓	✗	○	✓	✓	0 ↓
006	39Y/F	✓	✗	○○○○	✓	✓	2 ↓
007	48Y/F	✓	✓	○○○○○○	✓	✗	2 ↑
008	51Y/F	✓	✗	○○○	✓	✓	2 ↓
009	28Y/F	✓	✓	○○○○	✓	✓	1 ↓
010	31Y/F	✓	✓	○	✓	✓	1 ↓
011	56Y/M	✓	✓	○	✓	✓	1 ↓
012	36Y/F	✓	✓	○	✓	✓	2 ↓

Figure 5. Illustrates the patient-wise treatment strategy and follow-up up to a maximum of 24 months.

(105 ± 3.2 mg/dL). Hypothyroidism was identified in six female patients. PACNS-specific panels were negative across all patients, a critical finding given the initial clinical suspicions of MMS or central nervous system vasculitis and the subsequent ineffectiveness of immunosuppressive therapies. Electroencephalograms conducted in patients presenting with seizures did not reveal significant abnormalities beyond expected patterns.

Neuroimaging findings and angiographic landscape

Initial MRI/MRA (TOF) and CT/CTA assessed brain involvement and carotid fork irregularities, followed by six-vessel DSA confirmation, optimizing efficiency. CT/MR perfusion aided hemodynamics assessment in some cases. DSA revealed bilateral carotid fork involvement in 91.7% ($n = 11$), with unilateral left M1 segment of the MCA narrowing in one (ID-006). Bilateral M1 segment of the MCA involvement occurred in nine cases, four of which had concurrent bilateral A1-ACA and terminal ICA stenosis. Isolated bilateral terminal ICA or supraclinoid ICA narrowing was seen in one each. No “puff-of-smoke” collaterals were observed, leading neuroradiologists to suggest the possibility of “central nervous system vasculitis” (Table 3, Figure 2A1–D6; Supplementary File).

Results of next-generation sequencing and data analysis

Of 12 patients, 9 had the p.R4810K (c.14576G > A) RNF213 variant (75%), 1 had p.R4708C (ID-005), 1 had p.R4810K plus p.V1529M (ID-008) and 1 had p.R4859K (Isoform 1) (Table 4). Variants with minor allele frequency $<1 \times 10^{-3}$ were rare, including novel p.R4708C (c.14122C > T) and p.V1529M (c.4585G > A) (Figure 3A–B, Supplementary File). Among p.R4810K cases, 88.9% ($n = 8$) were heterozygous, and one was homozygous. Variants spanned Isoform 1 (p.R4859K) and Isoform 3 (p.R4810K, novel), likely de novo. Pathogenicity scores (PANTHER, CADD, Polyphen2, ClinVar) are shown in Figure 3C.

Clinical insights from treatment timeline

According to the AHA/ASA guidelines,²¹ all 12 received acute stroke care, transitioning to high-dependency units. Four received antiplatelets alone (2 with 1 recurrence, 2 with ≥ 3), while 8 received antiplatelets plus immunosuppression (5 with 1, 1 with 2, 2 with ≥ 3 recurrences) (Figure 4A–B, Figure 5), showing no benefit. Nine of 11 underwent EC-IC bypass (5 superficial temporal artery to MCA, 2 EDAMS, 2 combined), with no operated-side stroke recurrence and improved outcomes (Figure 4C, Figure 5). Two declined surgeries: ID-007 had six stroke recurrences, and ID-003 worsened to mRS 4 (Figure 5).

Insights from structural modeling of RNF213

A homology model of RNF213 (Isoform 3, residues 421–5205) was constructed and refined using molecular dynamics simulations. Structural validation with PROCHECK revealed that 89.8% of residues resided within favored regions of the Ramachandran plot, indicating a reliable model. Secondary structure analysis showed that the protein comprised approximately 49% alpha-helices and 6.6% beta-strands (Figure 6A–F; Supplementary File).

Three RNF213 variants – Val1529Met, Arg4708Cys and Arg4810Lys – were analyzed for their impact on protein stability. ConSurf conservation analysis indicated that residues Val1529 and Arg4708 are highly conserved, suggesting that mutations at these positions may significantly affect protein function. In contrast, Arg4810 is less conserved, implying that the Arg4810Lys variant might have a subtler effect on protein stability (Figure 7A–F).

Discussion

MMD is a progressive cerebrovascular disorder characterized by steno-occlusive changes at the terminal portion of the ICAs and the development of abnormal vascular networks. The RNF213 gene, located on chromosome 17q25.3, has been identified as a major susceptibility gene for MMD, particularly the p.R4810K variant,

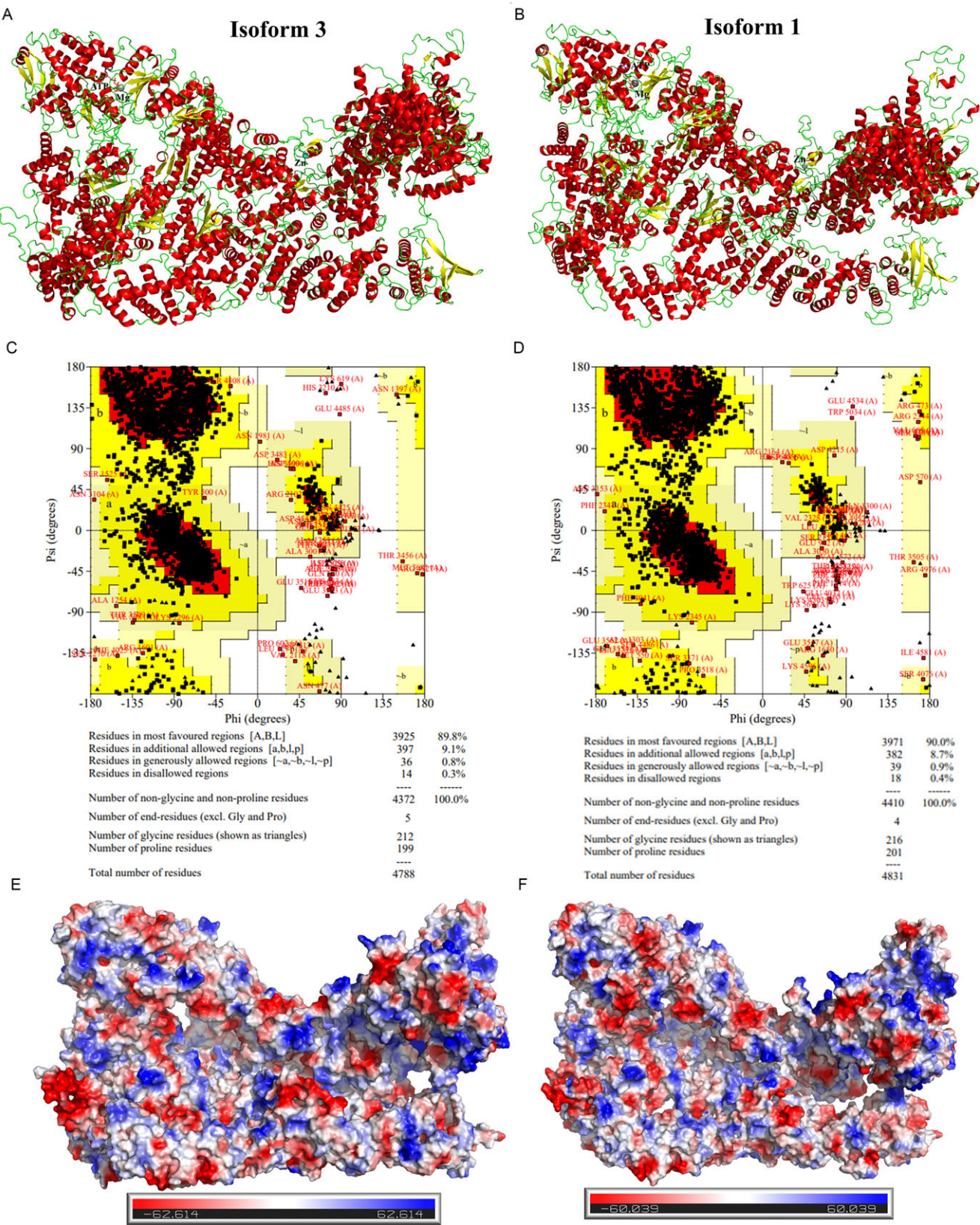


Figure 6. (A) Cartoon representation of human RN213 Isoform 3 (421-5205) and (B) Isoform 1 (427-5254). (C) and (D) demonstrate the Ramachandran plot statistics of human RN213 Isoforms 3 and 1, respectively. (E) and (F) illustrate the electrostatic distribution of human RN213 Isoforms 3 and 1, respectively.

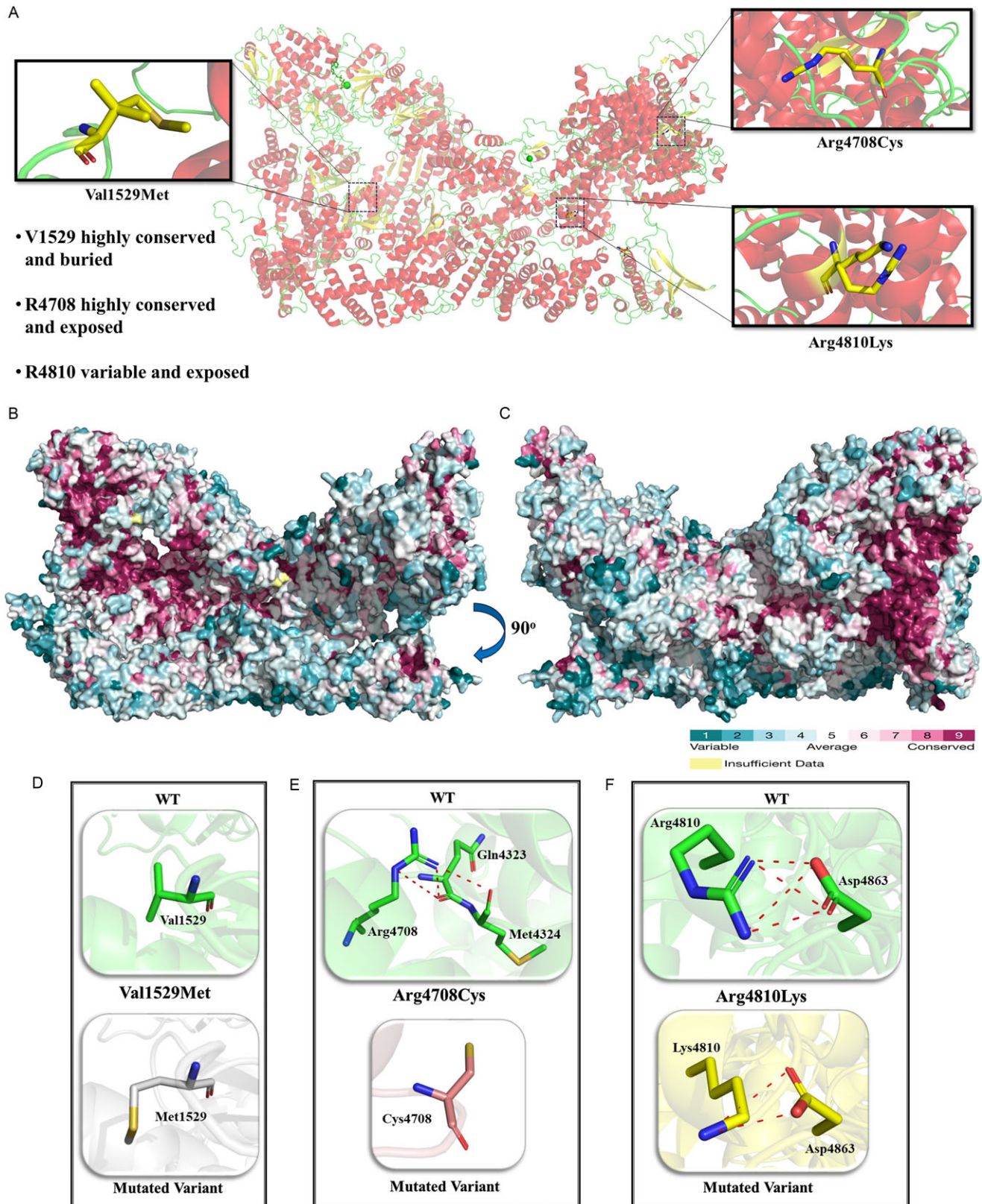


Figure 7. (A) Illustrates the mapping of different human RNF213 Isoform 3 variants. (B) and (C) demonstrate the surface representation of the evolutionary conservation of amino acid positions in human RNF213 Isoform 3 based on phylogenetic relations between homologous sequences. (D), (E) and (F) represent the residue interaction of wild-type (WT) and its variants in human RNF213 protein Isoform 3.

which is prevalent in East Asian populations.¹⁸ This variant has been associated with increased risk of MMD and other steno-occlusive diseases, including intracranial atherosclerotic disease (ICAD), pulmonary arterial hypertension and coronary artery disease.^{19–20}

In our study, we identified a cohort of patients exhibiting a unique “smokeless” phenotype of MMD, characterized by steno-occlusive changes at the carotid fork without the typical “puff-of-smoke” angiographic collaterals. All patients carried the RNF213 p.R4810K variant, with additional novel missense variants (p.V1529M, p.R4708C) identified in some cases. This phenotype challenges the conventional reliance on angiographic findings for MMD diagnosis and suggests that genetic testing for RNF213 variants can be instrumental in identifying such cases.

Differentiating “smokeless” MMD from ICAD is crucial, as their pathophysiological mechanisms and treatment responses differ.²¹ While ICAD is primarily managed with medical therapy, surgical revascularization remains the mainstay treatment for MMD.^{22–24} HR-VWI can aid in this differentiation; MMD typically presents with concentric, non-enhancing lesions and smaller outer diameters, whereas ICAD often shows eccentric plaques with wall enhancement and larger outer diameters. However, HR-VWI is not without limitations. There can be overlapping imaging features between MMD and ICAD, leading to potential misinterpretations.²⁵ For instance, both conditions may exhibit vessel wall enhancement, and the presence of such findings alone may not conclusively distinguish between them. Given these challenges, incorporating genetic testing, particularly for RNF213 variants like p.R4810K, can enhance diagnostic accuracy. RNF213 mutations are strongly associated with MMD, especially in East Asian populations, and their presence can support the diagnosis in cases where imaging findings are inconclusive.¹⁸ Early genetic testing can prevent misdiagnosis, avoid unnecessary treatments and guide appropriate surgical interventions.

The absence of basal collaterals in “smokeless” MMD raises questions about the underlying molecular mechanisms. Classical moyamoya vessels arise from the remodeling and dilation of pre-existing penetrating arteries, a process involving both arteriogenesis and angiogenesis.²⁶ RNF213 is believed to play a role in angiogenesis, and mutations in this gene may disrupt normal vascular remodeling. Studies have shown that RNF213-mediated angiogenesis may be an intrinsic phenomenon, independent of hypoxia-driven mechanisms.^{27–28}

In our cohort, all patients who underwent revascularization surgery ($n = 9$) demonstrated favorable postoperative outcomes, including improved mRS scores and no stroke recurrence at the operated side. These findings underscore the efficacy of surgical intervention in “smokeless” MMD cases.

Our study has several limitations. First, it was conducted with a limited sample size, which may affect the generalizability of our findings. Second, all patients were enrolled from a single center, potentially introducing selection bias. Third, due to ethical constraints, we could not perform genomic, transcriptomic and proteomic analyses on intracranial vascular samples, which could have provided further insights into the molecular basis of this novel phenotype. Future studies should aim to overcome these limitations by incorporating larger, multicenter cohorts and comprehensive molecular investigations.

Our findings underscore the existence of a “smokeless” MMD phenotype associated with RNF213 variants, reinforcing the diagnostic value of genetic testing in patients with steno-occlusive changes lacking characteristic angiographic collaterals. As

genetic testing transitions from research to routine clinical application, it is important to consider both turnaround time and cost. In our setting, concurrent moyamoya-targeted exome sequencing typically returns results within two weeks – well within the decision-making window for revascularization, particularly in adult cases. The cost, ranging from USD 110 to 130, is considered reasonable given the potential for genetic findings to inform diagnosis, avoid misclassification and prevent inappropriate therapies such as unwarranted immunosuppression. Early recognition of this phenotype may optimize patient management by guiding timely surgical intervention and improving long-term outcomes.

Conclusion

“Smokeless” MMD, marked by carotid fork steno-occlusion without classic basal collaterals, often mimics other vasculopathies, leading to diagnostic uncertainty. Incorporating RNF213 genetic testing alongside vessel wall imaging enhances diagnostic accuracy, distinguishing “smokeless” MMD from conditions like ICAD or PACNS. Early identification enables timely surgical revascularization, aligning treatment with classical MMD protocols and improving patient outcomes.

Supplementary material. The supplementary material for this article can be found at <https://dx.doi.org/10.1017/cjn.2025.10371>.

Data availability. Anonymized data supporting this study’s findings will be made available upon reasonable request to Dr Jayanta Roy (jroyneuro01@gmail.com) for researchers with appropriate qualifications.

Acknowledgments. The authors would like to acknowledge Professor Avik Roy Chowdhury from the Department of Laboratory Medicine for seamless efforts in managing all the lab reports and his views. We would also acknowledge the combined efforts of the medical records division, technicians of the MRI division and the CathLab team. Finally, we would like to express our gratitude toward our patients and their family members for the support they have given toward the fulfillment of this work.

Author contributions. J.R. contributed to (1) the conception organization of the study and (2) the writing of the first draft of the manuscript; S.D. contributed to (1) the conception organization of the study and (2) the writing of the first draft of the manuscript; R.M. contributed to (1) the conception organization of the study and (2) the writing of the first draft of the manuscript; G.S. contributed to collaborated on (1) the conception, organization and execution of the research project and (2) the review and critique of the manuscript; B.M. contributed to collaborated on (1) the conception, organization and execution of the research project and (2) the review and critique of the manuscript; M.T. contributed to collaborated on (1) the conception, organization and execution of the research project and (2) the review and critique of the manuscript; N.R. contributed to collaborated on (1) the conception, organization and execution of the research project and (2) the review and critique of the manuscript; A.S. contributed to collaborated on (1) the conception, organization and execution of the research project and (2) the review and critique of the manuscript; S.P. contributed to collaborated on (1) the conception, organization and execution of the research project and (2) the review and critique of the manuscript; P.S. contributed to collaborated on (1) the conception, organization and execution of the research project and (2) the review and critique of the manuscript; S.B. contributed to collaborated on (1) the conception, organization and execution of the research project and (2) the review and critique of the manuscript; A.M. contributed to collaborated on (1) the conception, organization and execution of the research project and (2) the review and critique of the manuscript; J.B.-L. contributed to collaborated on (1) the conception, organization and execution of the research project and (2) the review and critique of the manuscript; M.H. contributed to collaborated on (1) the conception, organization and execution of the research project and (2) the review and critique of the manuscript; S.H. contributed to collaborated on (1) the conception, organization and execution

of the research project and (2) the review and critique of the manuscript. All authors have reviewed and approved the final manuscript.

Funding statement. This study has been supported by institutional intramural funding. Julián Benito-León is supported by the National Institutes of Health (NINDS #R01 NS39422 and R01 NS094607) and the Recovery, Transformation, and Resilience Plan of the Spanish Ministry of Science and Innovation (grant TED2021-130174B-C33 and NETremor and grant PID2022-138585OB-C33, Resonate).

Competing interests. The authors declare that they have no competing interests.

References

- Kuroda S, Fujimura M, Takahashi J, et al. Diagnostic criteria for moyamoya disease - 2021 revised version. *Neurol Med-CHIR*. 2022;62(7):307–312.
- Suzuki J, Takaku A. Cerebrovascular “moyamoya” disease. Disease showing abnormal net-like vessels in base of brain. *Arch Neurol*. 1969;20(3):288–299.
- Gonzalez NR, Amin-Hanjani S, Bang OY, et al. Adult Moyamoya disease and syndrome: current perspectives and future directions: a scientific statement from the American Heart Association/American Stroke Association. *Stroke*. 2023;54(10):e465–e479.
- Morikawa R, Suzuki J, Nakai N, Takasu S, Itoh T, Ito Y. Moyamoya disease mimicking primary central nervous system vasculitis: a case report. *Med Case Rep Stud Protoc*. 2023;4(9):e00287.
- von Elm E, Altman DG, Egger M, Pocock SJ, Gøtzsche PC, Vandenbroucke JP. The strengthening the reporting of observational studies in epidemiology (STROBE) statement: guidelines for reporting observational studies. *Lancet (London, England)*. 2007;370(9596):1453–1457.
- Adzhubei IA, Schmidt S, Peshkin L, et al. A method and server for predicting damaging missense mutations. *Nat Methods*. 2010;7(4):248–249.
- Tang H, Thomas PD. PANTHER-PSEP: predicting disease-causing genetic variants using position-specific evolutionary preservation. *Bioinformatics (Oxford, England)*. 2016;32(14):2230–2232.
- Landrum MJ, Lee JM, Benson M, et al. ClinVar: public archive of interpretations of clinically relevant variants. *Nucleic Acids Res*. 2016;44(D1):D862–D868.
- Rentzsch P, Witten D, Cooper GM, Shendure J, Kircher M. CADD: predicting the deleteriousness of variants throughout the human genome. *Nucleic Acids Res*. 2019;47(D1):D886–D894.
- Altschul SF, Gish W, Miller W, Myers EW, Lipman DJ. Basic local alignment search tool. *J Mol Biol*. 1990;215(3):403–410.
- Crespillo-Casado A, Pothukuchi P, Naydenova K, et al. Recognition of phylogenetically diverse pathogens through enzymatically amplified recruitment of RNF213. *Embo Rep*. 2024;25(11):4979–5005.
- Webb B, Sali A. Comparative protein structure modeling using MODELLER. *Curr Protoc Bioinformatics*. 2016;54:5. 6. 1–5. 6. 37.
- Biasini M, Bienert S, Waterhouse A, et al. SWISS-MODEL: modelling protein tertiary and quaternary structure using evolutionary information. *Nucleic Acids Res*. 2014;42:W252–W258. (Web Server issue).
- Van Der Spoel D, Lindahl E, Hess B, Groenhof G, Mark AE, Berendsen HJ. GROMACS: fast, flexible, and free. *J Comput Chem*. 2005;26(16):1701–1718.
- Laskowski RA. PDBsum: summaries and analyses of PDB structures. *Nucleic Acids Res*. 2001;29(1):221–222.
- Emsley P, Cowtan K. Coot: model-building tools for molecular graphics. *Acta Crystallogr Section D Biol Crystallogr*. 2004;60(Pt 12 Pt 1):2126–2132.
- Ashkenazy H, Abadi S, Martz E, et al. ConSurf 2016: an improved methodology to estimate and visualize evolutionary conservation in macromolecules. *Nucleic Acids Res*. 2016;44(W1):W344–W350.
- Kamada F, Aoki Y, Narisawa A, et al. A genome-wide association study identifies RNF213 as the first Moyamoya disease gene. *J Hum Genet*. 2011;56(1):34–40.
- Yoshimoto T, Tanaka K, Koge J, et al. Impact of the <i>p.R4810K</i> variant on endovascular therapy for large -Vessel occlusion stroke. *Stroke Vasc Interv Neurol*. 2022;2(6):e000396.
- Suzuki H, Kataoka M, Hiraide T, et al. Genomic comparison with supercentenarians identifies RNF213 as a risk gene for pulmonary arterial hypertension. *Circ Genom Precis Med*. 2018;11(12):e002317.
- Guey S, Tournier-Lasserre E, Hervé D, Kossorotoff M. Moyamoya disease and syndromes: from genetics to clinical management. *Appl Clin Genet*. 2015;8:49–68.
- Grubb RL Jr., Powers WJ, Clarke WR, Videen TO, Adams HP Jr., Derdeyn CP. Surgical results of the carotid occlusion surgery study. *J Neurosurg*. 2013;118(1):25–33.
- Marshall RS, Festa JR, Cheung YK, et al. Randomized evaluation of carotid occlusion and neurocognition (RECON) trial: main results. *Neurology*. 2014;82(9):744–751.
- Komotar RJ, Starke RM, Otten ML, et al. The role of indirect extracranial-intracranial bypass in the treatment of symptomatic intracranial atheroocclusive disease. *J Neurosurg*. 2009;110(5):896–904.
- Kathuveetil A, Sylaja PN, Senthilvelan S, Kesavadas C, Banerjee M, Jayanand Sudhir B. Vessel wall thickening and enhancement in high-resolution intracranial vessel wall imaging: a predictor of future ischemic events in Moyamoya disease. *AJNR*. 2020;41(1):100–105.
- Liu J, Wang Y, Akamatsu Y, et al. Vascular remodeling after ischemic stroke: mechanisms and therapeutic potentials. *Prog Neurobiol*. 2014;115:138–156.
- Ye F, Niu X, Liang F, et al. RNF213 loss-of-function promotes pathological angiogenesis in moyamoya disease via the Hippo pathway. *Brain : a J Neurol*. 2023;146(11):4674–4689.
- Chen Y, Tang M, Li H, Liu H, Wang J, Huang J. TGFβ1 as a predictive biomarker for collateral formation within ischemic Moyamoya disease. *Front Neurol*. 2022;13:899470.